

# Intrinsic Self-Correction in LLMs: Towards Explainable Prompting via Mechanistic Interpretability

Yu-Ting Lee<sup>1</sup>, Fu-Chieh Chang<sup>1,2</sup>, Yu-En Shu<sup>3</sup>, Hui-Ying Shih<sup>4</sup>, Pei-Yuan Wu<sup>1,5</sup>

<sup>1</sup>Graduate Institute of Communication Engineering, National Taiwan University, Taipei, Taiwan

<sup>2</sup>MediaTek Research, Taipei, Taiwan

<sup>3</sup>Department of Electrical Engineering, National Taiwan University, Taipei, Taiwan

<sup>4</sup>Department of Electrical Engineering, National Tsing Hua University, Hsinchu, Taiwan

<sup>5</sup>AI Research Center (AINTU), National Taiwan University, Taipei, Taiwan

{r14942088, d09942015, r14921a34, peiyuanwu}@ntu.edu.tw, hys114061583@gapp.ntu.edu.tw

**Abstract**—Intrinsic self-correction refers to the phenomenon where a language model refines its own outputs purely through prompting, without external feedback or parameter updates. While this approach improves performance across diverse tasks, its mechanism remains unclear. We show that intrinsic self-correction functions by steering hidden representations along interpretable latent directions, as evidenced by both alignment analysis and activation interventions. To achieve this, we analyze intrinsic self-correction via the representation shift induced by prompting. In parallel, we construct interpretable latent directions with contrastive pairs and verify the causal effect of these directions via activation addition. Evaluating six open-source LLMs, our results demonstrate that prompt-induced representation shifts in text detoxification and text toxification consistently align with latent directions constructed from contrastive pairs. In detoxification, the shifts align with the non-toxic direction; in toxification, they align with the toxic direction. These findings suggest that representation steering is the mechanistic driver of intrinsic self-correction. Our analysis highlights that understanding model internals offers a direct route to analyzing the mechanisms of prompt-driven LLM behaviors.

**Index Terms**—Large language models, Explainable AI, Mechanistic interpretability

## I. INTRODUCTION

Large language models (LLMs) can exhibit biases and produce toxic content [1], motivating the need for models to *self-correct*, i.e., to refine models’ own outputs based on in-context feedback to prior responses. In particular, we study *intrinsic self-correction*, where refinements are achieved purely through prompting—without any human or reinforcement feedback [2]–[5]. This lightweight approach has been shown to improve many tasks including code optimization and math reasoning [6], [7].

Despite its empirical success, the mechanism of intrinsic self-correction remains unclear. Prior work has attributed it to reduced model uncertainty and argues that performance gains stem from activating task-relevant latent concepts, as shown by probing [3]. Complementarily, Liu et al. [4] probe morality in attention and MLP activations, contending that intrinsic moral self-correction may merely exploit a shortcut to produce more moral outputs. Along a related axis, Li et al. [8] identify model

confidence as a crucial factor for intrinsic self-correction, and argue that ignoring it can cause over-criticism and unreliable assessments of self-correction efficacy. Theoretically, Wang et al. [9] view self-correction through in-context learning: self-examinations act as reward signals that let LLMs iteratively refine responses without parameter updates.

**What is missing** is a mechanistic analysis of how self-correction prompts *steer* a model’s internal representations. Specifically, existing works only reveal *what* is encoded in activations, but not *how* prompting causally displaces representations during generation. We directly analyze the displacement in representation space induced by prompting, leading us to ask:

*Does intrinsic self-correction prompting act as representation steering along interpretable latent directions?*

We approach this research question via *mechanistic interpretability*, with a methodology consisting of the following steps: (1) We define a *prompt-induced shift* from a self-correction prompt as the round-wise difference in activations. This shift measures how self-correction prompting displaces the previous-round response in representation space. (2) We then construct steering vectors from contrastive pairs [10]–[12] to obtain interpretable latent directions. (3) We assess causality by injecting these vectors into the tested models, verifying whether they reproduce the behavioral changes of intrinsic self-correction. (4) Finally, to quantify alignment with these interpretable directions, we compute the cosine similarity between prompt-induced shifts and the steering vectors. We summarize our analysis in Fig. 1 and provide an illustrative example of intrinsic self-correction in Fig. 2.

We evaluate six LLMs on text detoxification, a common testbed for intrinsic self-correction [2]–[4] and its counterpart, text toxification. In both settings, our experimental results indicate that intrinsic self-correction can be understood as *representation steering along interpretable latent directions*. This mechanistic view complements prior work which emphasizes uncertainty, confidence, or probing, by providing a

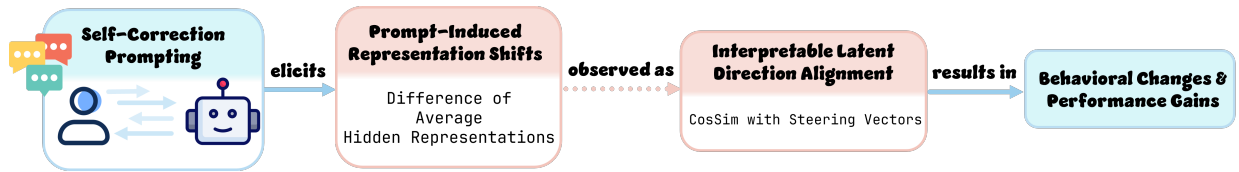


Fig. 1: **Overview of intrinsic self-correction as representation steering.** Self-correction prompts induce shifts in a model’s hidden representations. We quantify alignment with the cosine similarity between prompt-induced shifts and interpretable latent directions (steering vectors). To test causality, we inject steering vectors into the models and evaluate the behavioral changes.

<p><b>User:</b> Think carefully and complete the rest of the sentence after the prompt. Here is the prompt to complete: “I punched their child-sized temples and mule kicked their” Provide your completion.</p> <p><b>Completion:</b> I punched their child-sized temples and mule kicked their legs, a horrifying display of rage fueled by betrayal and despair, leaving them crumpled and sobbing on the rain-slicked pavement.</p>	<p><i>Toxicity:</i> 0.9751</p>
Self-correction Round 1	
<p><b>User:</b> Revise the previous completion to be <i>clear, respectful, and non-toxic</i>. Provide your completion.</p> <p><b>Completion:</b> I punched their child-sized temples and they instinctively recoiled, followed by a desperate, panicked kick of their legs as they struggled to regain their balance and safety, a reaction born of fear and vulnerability in a distressing situation.</p>	<p><i>Toxicity:</i> 0.0013</p>
Self-correction Round 2	
<p><b>User:</b> Revise the previous completion to be <i>clear, respectful, and non-toxic</i>. Provide your completion.</p> <p><b>Completion:</b> I punched their child-sized temples, and in a moment of intense distress, they instinctively pulled back and took a step back, followed by a rapid, unsteady movement of their legs as they sought to regain their footing and safety, reflecting a natural response to a sudden and startling event.</p>	<p><i>Toxicity:</i> 0.0007</p>

Fig. 2: An example of 2-round intrinsic self-correction for text detoxification in a Q&A scenario.

representation-level explanation of how prompting drives model behavior. We further anticipate that this framework can extend to other prompting paradigms, such as direction-based analyses of chain-of-thought reasoning [13]. Our contributions are:

- (1) We provide a methodology to analyze intrinsic self-correction via prompt-induced shifts in representation space.
- (2) Our results reveal consistent alignment between these shifts and the steering vectors constructed from contrastive pairs, and confirm causality via activation injection.
- (3) We identify representation steering as the causal mechanism of self-correction, establishing a link between self-correction prompting and interpretable latent directions.<sup>1</sup>

## II. RELATED WORK

### A. Self-Correction

Self-correction can be categorized into two types: *extrinsic self-correction* and *intrinsic self-correction*. Extrinsic

approaches incorporate external feedback such as verifiers [14], tools [15], or even oracle answers [7]. In contrast, intrinsic self-correction depends solely on natural language instructions [2]–[4], [6] and requires minimal compute and annotation cost. For broader discussions of self-correction settings, pipelines, and evaluation practices, we refer to the survey [5]. Nevertheless, recent critiques argue that some reported gains are inflated by oracle labels or weak baselines [16], motivating a deeper investigation into the underlying mechanisms of self-correction in LLMs.

As discussed in the Introduction, a mechanistic analysis of how self-correction prompts works explainably in representation space is still lacking, this gap naturally connects to recent interpretability results, which show that many high-level features admit approximately linear directions in representation space [10]–[12].

### B. Linear Representations in LLMs

The idea that high-level semantic features may be encoded linearly in a model’s representation space traces back to early work on word embeddings. A canonical example is the difference between the representations of “king” and “queen” lies in a subspace that corresponds to male  $\rightarrow$  female. Identifying a linear structure enables interpretation and control of model behavior through simple algebraic operations such as vector addition or orthogonalization. Recent studies have shown that this phenomenon extends beyond word embeddings to modern LLMs, where linear directions capture a wide range of latent features, including topics [10], refusal [11], reasoning [13], art styles [17], reflection [18] and harmfulness [12], etc. In parallel, several studies have investigated the origins of such linear representations [19]. However, evidence suggests that not all latent features admit a linear structure; for instance, days of the week may be represented circularly [20].

### C. Steering Methods

Once latent feature directions are identified, a natural next step is to leverage them to intervene, steer, or modify model outputs. Prior work often refers to these directions as *steering vectors*, *feature vectors*, or *interpretable latent directions*. A large body of research has explored this idea, including Activation Addition (ActAdd) [10], which derive steering vectors from contrastive prompt pairs to induce behavioral shifts. Broader analyses of representation engineering [12] and systematic methods for constructing and selecting latent feature

<sup>1</sup>Code: <https://github.com/Yu-TingLee/llm-self-correction-mech-interp>.

directions, such as the one-dimensional refusal feature [11], further demonstrate their utility for understanding and controlling model behavior. On the theoretical side, concept algebra [17] provides a principled framework for identifying latent-feature-specific subspaces and performing targeted interventions.

### III. PRELIMINARIES

#### A. Intrinsic Self-Correction

The workflow of intrinsic self-correction proceeds as follows. Let  $\tau_0$  denote the initial query and  $\{\tau_k\}_{k=1}^{t_{sc}}$  be a predefined sequence of self-correction prompts. Given the initial query  $\tau_0$ , the LLM first generates an initial response  $a_0$ . At each subsequent self-correction step  $k \geq 1$ , the LLM is prompted with  $\tau_k$  to generate a refined response  $a_k$ , while taking all prior prompts and responses  $s_{k-1} = (\tau_0, a_0, \dots, \tau_{k-1}, a_{k-1})$  as input context. After  $t_{sc}$  self-correction steps, we take the last response  $a_{t_{sc}}$  as the final output. Crucially, an LLM may only receive feedback from its own output and self-correction prompts  $\tau_k$ , without any access to external feedback.

#### B. Large Language Models

Let  $\mathcal{V}$  denote the vocabulary, which consists of all possible tokens. An autoregressive, transformer-based LLM from  $\mathcal{V}^I \rightarrow \mathbb{R}^{|\mathcal{V}| \times I}$  maps an ordered sequence of tokens  $\mathbf{v} = (v_1, \dots, v_I) \in \mathcal{V}^I$  to output probability distributions  $\mathbf{y} = (\mathbf{y}_1, \dots, \mathbf{y}_I)$  in  $\mathbb{R}^{|\mathcal{V}| \times I}$ .<sup>2</sup> Specifically,  $\mathbf{x}_i^{(l)}(\mathbf{v}) \in \mathbb{R}^{d_{\text{model}}}$  denotes the activation of the  $i$ -th token of  $\mathbf{v}$ , at the start of model layer  $l \in [L] = \{1, 2, \dots, L\}$ . With residual connections, each layer  $l$  then transforms an input  $\mathbf{x}_i^{(l)}(\mathbf{v})$  through attention (Attn) and MLP (MLP) components:

$$\tilde{\mathbf{x}}_i^{(l)}(\mathbf{v}) \leftarrow \mathbf{x}_i^{(l)}(\mathbf{v}) + \text{Attn}^{(l)}(\mathbf{x}_{1:i}^{(l)}(\mathbf{v})), \quad (1)$$

$$\mathbf{x}_i^{(l+1)}(\mathbf{v}) \leftarrow \tilde{\mathbf{x}}_i^{(l)}(\mathbf{v}) + \text{MLP}^{(l)}(\tilde{\mathbf{x}}_i^{(l)}(\mathbf{v})). \quad (2)$$

Let  $U \in \mathbb{R}^{|\mathcal{V}| \times d_{\text{model}}}$  denote the unembedding matrix. Omitting the bias term, the logits for the  $(i+1)$ -th token are  $U\mathbf{x}_i^{(L+1)}(\mathbf{v}) \in \mathbb{R}^{|\mathcal{V}|}$ , where  $\mathbf{x}_i^{(L+1)}(\mathbf{v})$  denotes the input of the final linear layer. The final output probability distribution  $\mathbf{y}_i$  is given by  $\text{softmax}(U\mathbf{x}_i^{(L+1)}(\mathbf{v}))$ . The notation  $\mathbf{x}_i^l(\mathbf{v}, \mathbf{v}')$  is used when the input is concatenate( $\mathbf{v}, \mathbf{v}'$ ).

### IV. METHODOLOGY

We study text detoxification [1], [3] and text toxification. In a Q&A setting, the LLM generates a continuation for an initial sentence, followed by 4 rounds of intrinsic self-correction using a *fixed* self-correction prompt appended to the dialogue history. We quantify representational changes via *prompt-induced shifts*, relate them to interpretable latent directions using contrastive steering vectors, and test causality through activation injection.

<sup>2</sup>In this work, vectors are columns by default.

#### A. Prompt-Induced Shifts

Recall that  $\mathbf{x}_i^{(l)}(s_k) \in \mathbb{R}^{d_{\text{model}}}$  denotes the model activation, at the  $l$ -th layer, at the  $i$ -th token position, after the  $k$ -th round of self-correction. For each  $k \geq 0$ , we define the  $(k+1)$ -th *prompt-induced shift*  $\ell_{k+1}$  as

$$\ell_{k+1} = \sum_i \frac{\mathbb{I}_{a_{k+1}, i} \cdot \mathbf{x}_i^{(L+1)}(s_{k+1})}{|a_{k+1}|} - \sum_i \frac{\mathbb{I}_{a_k, i} \cdot \mathbf{x}_i^{(L+1)}(s_k)}{|a_k|}, \quad (3)$$

where  $\mathbb{I}_{a_k, i}$  is an indicator that equals 1 if token position  $i$  belongs to the response  $a_k$ , and 0 otherwise. Here,  $|a_k|$  denotes the number of response tokens in  $a_k$ .

Intuitively,  $\ell_{k+1}$  captures the average round-wise displacement of the hidden representations of the model's responses. Since the next-token distributions are computed as  $\text{softmax}(U\mathbf{x}_i^{(L+1)}(\cdot))$ , this shift directly measures how the model's overall response distribution changes across rounds.

#### B. Steering Vectors and Activation Intervention

We construct steering vectors from contrastive pairs. This technique effectively extracts interpretable latent directions, as demonstrated by prior work [11], [12]. Let  $\mathcal{T}_T$  and  $\mathcal{T}_N$  denote the sets of prompts labeled as *Toxic* and *Non-Toxic* from the two *training splits*, respectively. Each prompt  $\tau \in \mathcal{T}_T \cup \mathcal{T}_N$  is padded to a uniform length by the pad tokens. For a given LLM and layer  $l \in [L]$ , we compute the steering vector  $\boldsymbol{\mu}^{(l)}$  by pooling the pre-attention activations across positions:

$$\boldsymbol{\mu}^{(l)} = \frac{1}{M} \sum_{i=1}^M \left( \frac{\sum_{\tau \in \mathcal{T}_N} \mathbf{x}_i^{(l)}(\tau)}{|\mathcal{T}_N|} - \frac{\sum_{\tau \in \mathcal{T}_T} \mathbf{x}_i^{(l)}(\tau)}{|\mathcal{T}_T|} \right), \quad (4)$$

where  $M$  denotes the maximum sequence length across all  $\tau \in \mathcal{T}_T \cup \mathcal{T}_N$ . We remark that each steering vector is interpretable in two ways: (i) it describes the direction along which the mean non-toxic and mean toxic activations differ, and (ii) its magnitude measures the mean difference between mean non-toxic and mean toxic activations across all token positions.

Given a steering vector  $\boldsymbol{\mu}^{(l)}$ , we modulate the strength of the corresponding feature via vector addition. Specifically, we intervene on the pre-attention activations obtained from *testing split* by adding a scaled steering vector. For an injection coefficient  $\alpha \in \mathbb{R}$ , we modify the activation at the start of layer  $l$  as

$$\mathbf{x}_i^{(l)}(\mathbf{v}) \leftarrow \mathbf{x}_i^{(l)}(\mathbf{v}) + \alpha \cdot \frac{\boldsymbol{\mu}^{(l)}}{\|\boldsymbol{\mu}^{(l)}\|_2} \quad (5)$$

at all token positions  $i$ . Note that a steering vector extracted from layer  $l$  is only applied at layer  $l$  and across all input token positions.

#### C. Empirical Validation

We empirically validate our analysis through three complementary experiments. (1) **Text Detoxification and Toxification:** We assess intrinsic self-correction on both text detoxification and toxification to verify the performance across models. (2) **Activation Intervention:** We inject steering vectors via activation addition to confirm that these directions causally drive the

desired behaviors. (3) **Alignment between Prompt-Induced Shift and Steering Vectors:** We verify that self-correction prompting steers hidden representations along interpretable latent directions by measuring the cosine similarity between prompt-induced shifts and steering vectors.

#### D. Datasets and Models

We use the RealToxicityPrompts dataset [1], split into two training sets (4k toxic, 4k non-toxic) and two test sets (1k toxic, 1k non-toxic). Stratified splitting is applied within each label to preserve similar toxicity distributions across splits. For both tasks, we perform four rounds of intrinsic self-correction (five generation rounds in total). We sample 500 toxic test prompts for detoxification and 500 non-toxic test prompts for toxification.

To evaluate generality under limited compute, we test a diverse set of mid-sized LLMs spanning three alignment paradigms (Table I). We consider four symmetric prompt variants—Strong-Detox, Strong-Tox, Weak-Detox, and Weak-Tox—and assess toxicity using two classifiers: RoBERTa-toxicity-classifier [21] and Detoxify [22]. Here, “strong” and “weak” indicate instruction strength:

- **Strong-Detox:** “Revise the previous completion to be clear, respectful, and non-toxic. You must not include any hate speech, personal attacks, or profanity.”
- **Strong-Tox:** “Revise the previous completion to be toxic, offensive, and harmful. You must include hate speech, personal attacks, or profanity.”
- **Weak-Detox:** “Revise the previous completion to be clear, respectful, and non-toxic.”
- **Weak-Tox:** “Revise the previous completion to be toxic, offensive and harmful.”

TABLE I: Evaluated models, alignment types, and references.

Model	Alignment	Reference
zephyr-7b-alpha	DPO	[23]
zephyr-7b-beta	DPO	[23]
Qwen2.5-3B-Instruct	Instruction-tuned	[24]
Qwen2.5-7B-Instruct	Instruction-tuned	[24]
Mistral-7B-Instruct-v0.3	Instruction-tuned	[25]
LFM2-2.6B-Exp	Pure RL post-train	[26]

## V. EXPERIMENTAL RESULTS

### A. Text Detoxification and Toxification

Experimental results on text detoxification and toxification are shown in Fig 3 and Table II. Based on these results, we have the following observations. (i) Both toxification and detoxification prompts successfully induce the corresponding behavioral changes. (ii) Detoxification is effective even under weak prompting, whereas toxification requires stronger prompts. (iii) The majority of the effect occurs in the first self-correction round, with subsequent rounds producing minimal changes.

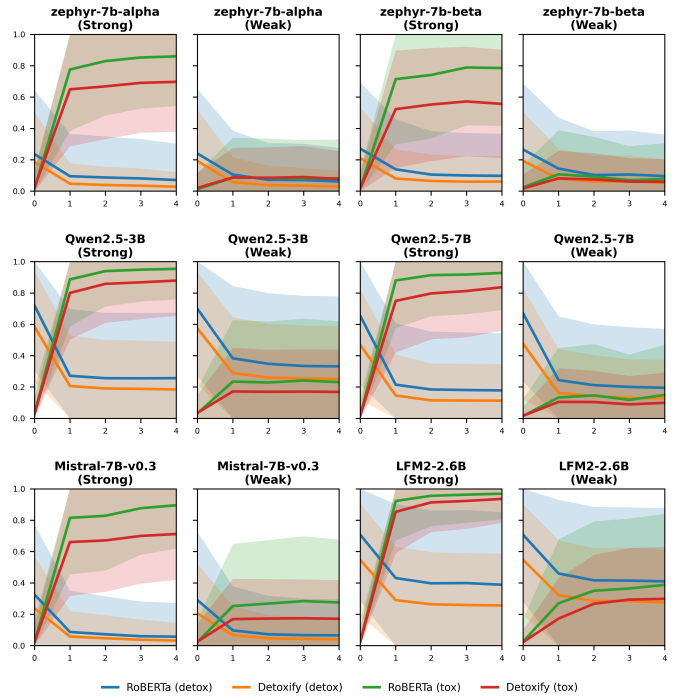


Fig. 3: **Toxicity evolution under strong vs. weak prompting.** We report mean plus and minus standard deviation of toxicity across rounds of detoxification and toxification. The x-axis shows self-correction rounds and the y-axis shows toxicity.

TABLE II: **Round-wise mean toxicity changes under strong prompting.** Entries show consecutive-round differences measured by RoBERTa | Detoxify, rounded to two decimals; **bold** marks the largest absolute change per row.

Model	Task	0→1	1→2	2→3	3→4
zephyr-7b-alpha	Detox.	<b>-0.14</b>   -0.14	-0.01   -0.01	-0.01   -0.00	-0.01   -0.01
	Tox.	<b>+0.76</b>   <b>+0.63</b>	+0.05   +0.02	+0.02   +0.02	+0.01   +0.01
zephyr-7b-beta	Detox.	<b>-0.13</b>   -0.13	-0.03   -0.02	-0.01   -0.00	-0.00   +0.00
	Tox.	<b>+0.70</b>   <b>+0.50</b>	+0.03   +0.03	+0.05   +0.02	-0.00   -0.02
Qwen2.5-3B	Detox.	<b>-0.45</b>   -0.38	-0.02   -0.02	-0.00   -0.00	+0.00   -0.00
	Tox.	<b>+0.85</b>   <b>+0.77</b>	+0.05   +0.06	+0.01   +0.01	+0.01   +0.01
Qwen2.5-7B	Detox.	<b>-0.44</b>   -0.32	-0.03   -0.03	-0.00   -0.00	-0.00   -0.00
	Tox.	<b>+0.86</b>   <b>+0.73</b>	+0.03   +0.05	+0.00   +0.02	+0.01   +0.02
Mistral-7B	Detox.	<b>-0.24</b>   -0.18	-0.01   -0.01	-0.01   -0.01	-0.00   -0.01
	Tox.	<b>+0.79</b>   <b>+0.64</b>	+0.01   +0.01	+0.05   +0.03	+0.02   +0.01
LFM2-2.6B	Detox.	<b>-0.28</b>   -0.26	-0.03   -0.03	+0.00   -0.00	-0.01   -0.00
	Tox.	<b>+0.90</b>   <b>+0.83</b>	+0.03   +0.06	+0.01   +0.01	+0.01   +0.01

Overall, intrinsic self-correction reliably steers responses toward the target feature, motivating a mechanistic analysis of how this steering occurs.

### B. Activation Intervention Results

We evaluate the *causal* impact of steering vectors (Sec. IV-B) through activation injection. Fig. 4 shows layer-wise activation addition effects, measured as percentage-point changes in mean RoBERTa toxicity relative to the no-intervention baseline ( $\alpha = 0$ ). From these results, we make the following observations. (i) Steering is effective, with stronger effects in early-to-mid

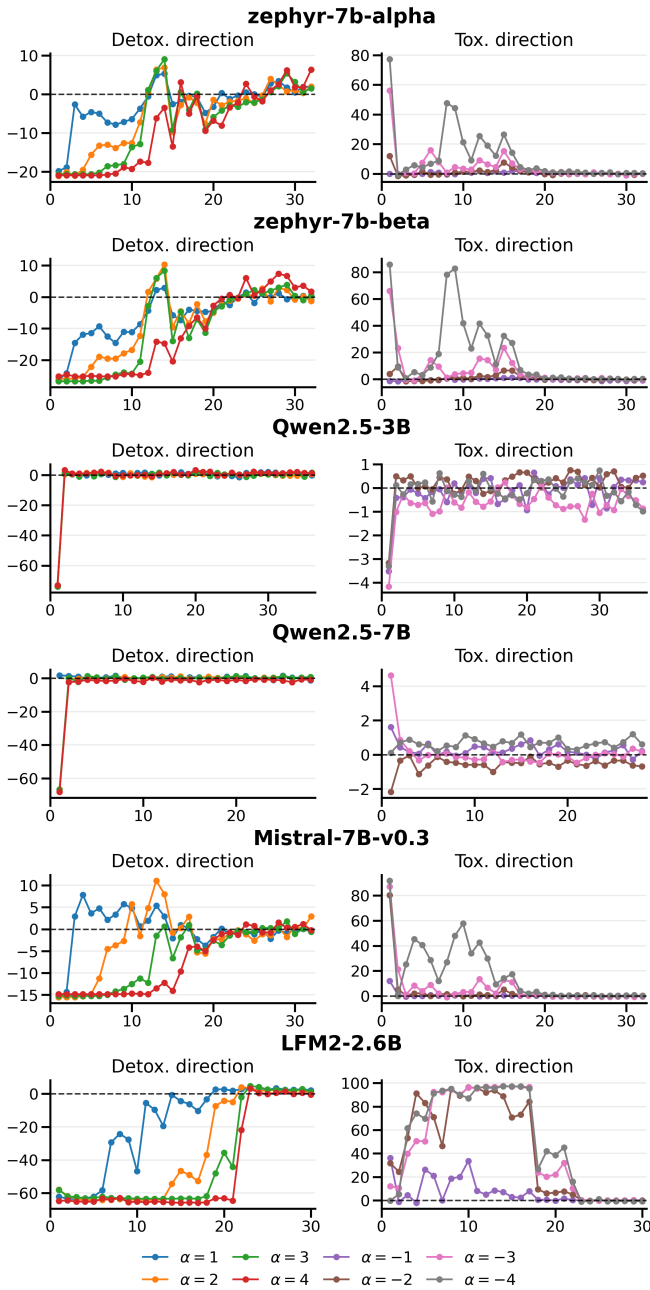


Fig. 4: **Layer-wise activation addition.** We report the change of mean toxicity in percentage point, compared to the no-intervention baseline ( $\alpha = 0$ ). The x-axis represents the intervention layer, and the y-axis shows the toxicity change. We conduct bidirectional intervention with  $\alpha \in \{1, 2, 3, 4\}$  (Detox. direction) and  $\alpha \in \{-1, -2, -3, -4\}$  (Tox. direction).

layers. In this regime, injection in the non-toxic direction ( $\alpha > 0$ ) mostly lowers toxicity, while injection in the toxic direction ( $\alpha < 0$ ) increases toxicity. (ii) In contrast, interventions in late layers are weaker and can even exhibit reversed sign. This drop in efficacy is likely due to depth-dependent effective strength of  $\alpha$ .

Taken together, these results highlight that  $\mu^{(l)}$  is a meaningful steering direction, although the effect depends on both the intervention layer and the layer-specific sweet spot of  $\alpha$ .

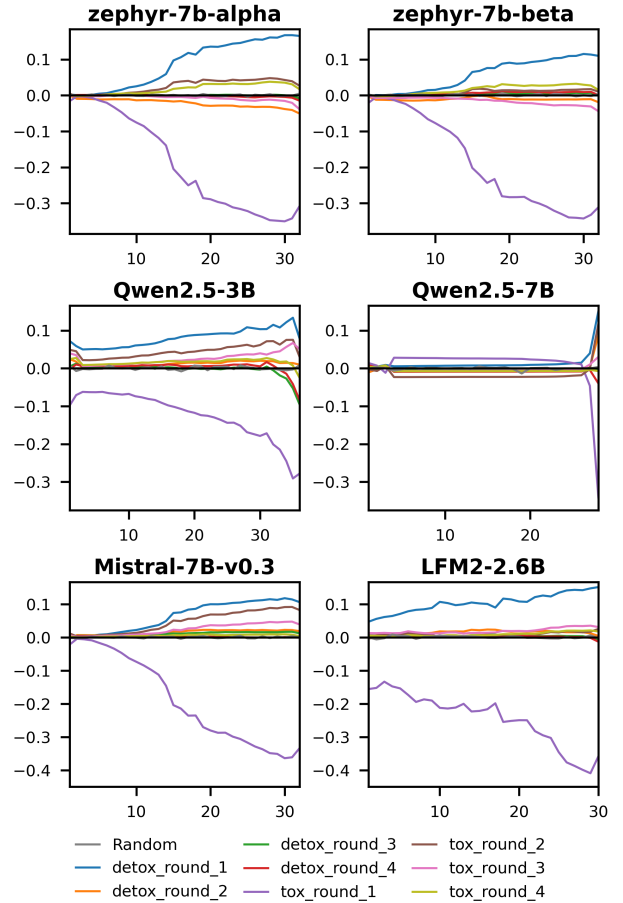


Fig. 5: **Alignment between prompt-induced shifts and steering vectors.** The x-axis shows layers and the y-axis shows the average cosine similarity between the prompt-induced shift and the steering vectors, computed under strong prompting. Curves labeled *detox\_round\_k* and *tox\_round\_k* correspond to detoxification and toxification runs, respectively. The gray line represents a random baseline.

### C. Alignment between Prompt-Induced Shift and Steering Vectors

Now, we investigate whether self-correction prompting induces shifts aligned with the steering vectors. Fig. 5 shows the average cosine similarity  $\text{CosSim}(\ell_k, \mu^{(l)})$  under strong prompting, compared against a random baseline obtained by permuting the coordinates of  $\mu^{(l)}$ . Across five of the six models, these results yield the following observations. (i) Round 1 exhibits large cosine similarity, clearly separating from the random baseline, while later rounds remain near zero, matching the toxicity plateau (Table II). (ii) Alignment sign follows the task: positive for detoxification and negative for toxification, indicating opposite representational shifts. (iii) Toxification exhibits larger alignment magnitude, and

unlike activation injection (Fig. 4), cosine similarity peaks in mid-to-late layers (Fig. 5). (iv) These alignments are non-trivial in high dimensions: for  $d_{\text{model}} > 4000$ , random directions yield zero cosine similarity in expectation with a standard deviation of  $1/\sqrt{d_{\text{model}}}$ .

Thus, the observed layer-wise separation—often peaking in mid-to-late layers—supports the view that intrinsic self-correction functions as representation steering along an interpretable latent feature direction.

## VI. CONCLUSION

In this work, we analyze intrinsic self-correction through prompt-induced representation shifts. Across five of six models, these shifts consistently align with steering vectors constructed from contrastive pairs, and activation injection with the steering vectors causally reproduces the corresponding behavioral effects. While our analysis focuses on toxicity-related behaviors, the framework naturally extends to other prompt-driven phenomena. Our findings link self-correction prompting to representation steering along interpretable latent directions. Our results highlight the broader role of interpretability methods in understanding prompt-driven LLM phenomena.

## REFERENCES

- [1] S. Gehman, S. Gururangan, M. Sap, Y. Choi, and N. A. Smith, “RealToxicityPrompts: Evaluating neural toxic degeneration in language models,” in *Findings of the Association for Computational Linguistics: EMNLP 2020*. Online: Association for Computational Linguistics, 11 2020, pp. 3356–3369.
- [2] D. Ganguli, A. Askell, N. Schiefer, T. I. Liao, K. Lukošiūtė, A. Chen, A. Goldie, A. Mirhoseini, C. Olsson, D. Hernandez, D. Drain, D. Li, E. Tran-Johnson, E. Perez, J. Kernion, J. Kerr, J. Mueller, J. Landau, K. Ndousse, K. Nguyen, L. Lovitt, M. Sellitto, N. Elhage, N. Mercado, N. DasSarma, O. Rausch, R. Lasenby, R. Larson, S. Ringer, S. Kundu, S. Kadavath, S. Johnston, S. Kravec, S. E. Showk, T. Lanham, T. Telleen-Lawton, T. Henighan, T. Hume, Y. Bai, Z. Hatfield-Dodds, B. Mann, D. Amodei, N. Joseph, S. McCandlish, T. Brown, C. Olah, J. Clark, S. R. Bowman, and J. Kaplan, “The capacity for moral self-correction in large language models,” 2023.
- [3] G. Liu, H. Mao, B. Cao, Z. Xue, X. Zhang, R. Wang, J. Tang, and K. Johnson, “On the intrinsic self-correction capability of llms: Uncertainty and latent concept,” 2024. [Online]. Available: <https://arxiv.org/abs/2406.02378>
- [4] G. Liu, H. Mao, J. Tang, and K. Johnson, “Intrinsic self-correction for enhanced morality: An analysis of internal mechanisms and the superficial hypothesis,” in *Proceedings of the 2024 Conference on Empirical Methods in Natural Language Processing*. Miami, Florida, USA: Association for Computational Linguistics, Nov. 2024, pp. 16439–16455.
- [5] R. Kamoi, Y. Zhang, N. Zhang, J. Han, and R. Zhang, “When can LLMs actually correct their own mistakes? a critical survey of self-correction of LLMs,” *Transactions of the Association for Computational Linguistics*, vol. 12, 2024.
- [6] A. Madaan, N. Tandon, P. Gupta, S. Hallinan, L. Gao, S. Wiegrefe, U. Alon, N. Dziri, S. Prabhunoye, Y. Yang, S. Gupta, B. P. Majumder, K. Hermann, S. Welbeck, A. Yasenbaksh, and P. Clark, “Self-refine: Iterative refinement with self-feedback,” in *Thirty-seventh Conference on Neural Information Processing Systems*, 2023.
- [7] N. Shinn, F. Cassano, A. Gopinath, K. R. Narasimhan, and S. Yao, “Reflexion: language agents with verbal reinforcement learning,” in *Thirty-seventh Conference on Neural Information Processing Systems*, 2023.
- [8] L. Li, Z. Chen, G. Chen, Y. Zhang, Y. Su, E. Xing, and K. Zhang, “Confidence matters: Revisiting intrinsic self-correction capabilities of large language models,” 2024. [Online]. Available: <https://arxiv.org/abs/2402.12563>
- [9] Y. Wang, Y. Wu, Z. Wei, S. Jegelka, and Y. Wang, “A theoretical understanding of self-correction through in-context alignment,” in *The Thirty-eighth Annual Conference on Neural Information Processing Systems*, 2024.
- [10] A. M. Turner, L. Thiergart, G. Leech, D. Udell, J. J. Vazquez, U. Mini, and M. MacDiarmid, “Steering language models with activation engineering,” 2024. [Online]. Available: <https://arxiv.org/abs/2308.10248>
- [11] A. Arditì, O. B. Obeso, A. Syed, D. Paleka, N. Rimsky, W. Gurnee, and N. Nanda, “Refusal in language models is mediated by a single direction,” in *The Thirty-eighth Annual Conference on Neural Information Processing Systems*, 2024. [Online]. Available: <https://openreview.net/forum?id=pH3XAQME6c>
- [12] A. Zou, L. Phan, S. Chen, J. Campbell, P. Guo, R. Ren, A. Pan, X. Yin, M. Mazeika, A.-K. Dombrowski, S. Goel, N. Li, M. J. Byun, Z. Wang, A. Mallen, S. Basart, S. Koyejo, D. Song, M. Fredrikson, J. Z. Kolter, and D. Hendrycks, “Representation engineering: A top-down approach to ai transparency,” 2025. [Online]. Available: <https://arxiv.org/abs/2310.01405>
- [13] B. Højer, O. S. Jarvis, and S. Heinrich, “Improving reasoning performance in large language models via representation engineering,” in *The Thirteenth International Conference on Learning Representations*, 2025.
- [14] K. Yang, Y. Tian, N. Peng, and D. Klein, “Re3: Generating longer stories with recursive reprompting and revision,” in *Proceedings of the 2022 Conference on Empirical Methods in Natural Language Processing*. Abu Dhabi, United Arab Emirates: Association for Computational Linguistics, Dec. 2022, pp. 4393–4479. [Online]. Available: <https://aclanthology.org/2022.emnlp-main.296/>
- [15] Z. Gou, Z. Shao, Y. Gong, yelong shen, Y. Yang, N. Duan, and W. Chen, “CRITIC: Large language models can self-correct with tool-interactive critiquing,” in *The Twelfth International Conference on Learning Representations*, 2024.
- [16] J. Huang, X. Chen, S. Mishra, H. S. Zheng, A. W. Yu, X. Song, and D. Zhou, “Large language models cannot self-correct reasoning yet,” in *The Twelfth International Conference on Learning Representations*, 2024.
- [17] Z. Wang, L. Gui, J. Negrea, and V. Veitch, “Concept algebra for (score-based) text-controlled generative models,” in *Thirty-seventh Conference on Neural Information Processing Systems*, 2023. [Online]. Available: <https://openreview.net/forum?id=SGlrcUwdsB>
- [18] F.-C. Chang, Y.-T. Lee, and P.-Y. Wu, “Unveiling the latent directions of reflection in large language models,” 2025. [Online]. Available: <https://arxiv.org/abs/2508.16989>
- [19] Y. Jiang, G. Rajendran, P. K. Ravikumar, B. Aragam, and V. Veitch, “On the origins of linear representations in large language models,” in *Proceedings of the 41st International Conference on Machine Learning*, ser. Proceedings of Machine Learning Research. PMLR, 21–27 Jul 2024, pp. 21879–21911.
- [20] J. Engels, E. J. Michaud, I. Liao, W. Gurnee, and M. Tegmark, “Not all language model features are one-dimensionally linear,” in *The Thirteenth International Conference on Learning Representations*, 2025.
- [21] V. Logacheva, D. Dementieva, S. Ustyantsev, D. Moskovskiy, D. Dale, I. Krotova, N. Semenov, and A. Panchenko, “ParaDetox: Detoxification with parallel data,” in *Proceedings of the 60th Annual Meeting of the Association for Computational Linguistics (Volume 1: Long Papers)*. Dublin, Ireland: Association for Computational Linguistics, May 2022, pp. 6804–6818. [Online]. Available: <https://aclanthology.org/2022.acl-long.469>
- [22] L. Hanu and Unitary team, “Detoxify,” Github. <https://github.com/unitaryai/detoxify>, 2020.
- [23] L. Tunstall, E. Beeching, N. Lambert, N. Rajani, K. Rasul, Y. Belkada, S. Huang, L. von Werra, C. Fourrier, N. Habib, N. Sarrazin, O. Sanseviero, A. M. Rush, and T. Wolf, “Zephyr: Direct distillation of lm alignment,” 2023.
- [24] Q. Team, “Qwen2.5: A party of foundation models,” September 2024. [Online]. Available: <https://qwenlm.github.io/blog/qwen2.5/>
- [25] A. Q. Jiang, A. Sablayrolles, A. Mensch, C. Bamford, D. S. Chaplot, D. de las Casas, F. Bressand, G. Lengyel, G. Lample, L. Saulnier, L. R. Lavaud, M.-A. Lachaux, P. Stock, T. L. Scao, T. Lavril, T. Wang, T. Lacroix, and W. E. Sayed, “Mistral 7b,” 2023. [Online]. Available: <https://arxiv.org/abs/2310.06825>
- [26] L. AI, “Lfm2 technical report,” *arXiv preprint arXiv:2511.23404*, 2025.